



Exploring ligand interactions with human phosphomannomutases using recombinant bacterial thermal shift assay and biochemical validation



Maria Monticelli ^{a, b}, Bruno Hay Mele ^b, Demi Marie Wright ^{a, c}, Simone Guerriero ^b,
Giuseppina Andreotti ^{a, *}, Maria Vittoria Cubellis ^{a, b, d}

^a Institute of Biomolecular Chemistry ICB, CNR, Via Campi Flegrei 34, 80078, Pozzuoli, Italy

^b Department of Biology, University of Napoli "Federico II", Complesso Universitario Monte Sant'Angelo, Via Cinthia, 80126, Napoli, Italy

^c Institute of Chemistry and Biochemistry, Freie Universität Berlin, D-14195, Berlin, Germany

^d Stazione Zoologica "Anton Dohrn", Villa Comunale, Naples, Italy

ARTICLE INFO

Article history:

Received 2 February 2024

Accepted 26 February 2024

Available online 6 March 2024

Handling Editor: Dr B Friguet

Keywords:

Protein-ligand binding

Protein stability

CeTSA

ReBaTSA

In silico docking

Phosphomannomutase-2

ABSTRACT

PMM2-CDG, a disease caused by mutations in phosphomannomutase-2, is the most common congenital disorder of glycosylation. Yet, it still lacks a cure. Targeting phosphomannomutase-2 with pharmacological chaperones or inhibiting the phosphatase activity of phosphomannomutase-1 to enhance intracellular glucose-1,6-bisphosphate have been proposed as therapeutical approaches.

We used Recombinant Bacterial Thermal Shift Assay to assess the binding of a substrate analog to phosphomannomutase-2 and the specific binding to phosphomannomutase-1 of an FDA-approved drug - clodronate. We also deepened the clodronate binding by enzyme activity assays and *in silico* docking. Our results confirmed the selective binding of clodronate to phosphomannomutase-1 and shed light on such binding.

© 2024 The Authors. Published by Elsevier B.V. This is an open access article under the CC BY-NC-ND license (<http://creativecommons.org/licenses/by-nc-nd/4.0/>).

1. Introduction

Small molecules can modulate the activity or stability of a target protein by acting as inhibitors, activators, or stabilizers [1]. Several techniques enable the screening of ligands for specific proteins, yet there is a high demand for simple and low-cost methods. Addressing this need, Thermal Shift Assay (TSA), Cellular Thermal Shift Assay (CeTSA) and Recombinant Bacterial Thermal Shift Assay (ReBaTSA) have emerged as novel techniques, leveraging the unique properties of specific ligands to stabilize their protein target upon binding [2–5]. These techniques have a broad range of applications in variant effect assessment in genetic disorders, as most missense mutations linked to disease affect protein stability rather than its function. Understanding how a drug interacts with and influences a protein, especially a pathological variant, becomes crucial in this context. A drug can enhance the stability of a

pathological variant either directly, by specific binding, or indirectly either by acting as a pharmacological chaperone or modulating protein degradation.

Phosphomannomutase-2 (PMM2, O15305) is an essential enzyme in the initial stages of protein glycosylation. Mutations in this enzyme cause PMM2-CDG, a genetic disorder that affects multiple organs, especially the central nervous system [6–9]. This disease is characterized by two distinct peculiarities: firstly, all patients retain some degree of residual enzymatic activity, as a complete loss of PMM2 function has been proven lethal. Secondly, no patient possesses two inactive alleles: in all cases, at least one allele produces an unstable yet functional protein [10–19]. The importance of this characteristic is related to the feasibility of stabilization-based treatments for PMM2-CDG, since a functional even though unstable protein is available in patients' cells. To this end, pharmacological chaperones (PCs) represent a promising and open approach. The principle behind it is that some small molecules (PCs) are able to stabilize the target protein through specific binding. Protein stability bears on the misfolded proteins degradation pathways, eventually contributing to restore physiological

* Corresponding author.

E-mail address: gandreotti@icb.cnr.it (G. Andreotti).

Abbreviations

α -G16	α -glucose-1,6-bisphosphate
β -G16	β -glucose-1,6-bisphosphate
CDG	congenital disorders of glycosylation
CeTSA	Cellular Thermal Shift Assay
G1P	glucose-1-phosphate
CL4	clodronate
G16	glucose-1,6-bisphosphate
M1P	mannose-1-phosphate
M6P	mannose-6-phosphate
PMM1	phosphomannomutase-1
PMM2	phosphomannomutase-2
ReBaTSA	Recombinant Bacterial Thermal Shift Assay

activity levels by stabilized mutant protein accumulation. Some potential pharmacological chaperones for PMM2-CDG have been identified, although they have not progressed to clinical trials, and the search for new drugs continues [13,15,18,20–22].

PMM2 catalyzes the isomerization of mannose-6-phosphate (M6P) to mannose-1-phosphate (M1P) and requires α -glucose-1,6-bisphosphate (α -G16) as a cofactor [20]. In addition to triggering enzymatic activity, α -G16 stabilizes both wild-type PMM2 and its pathological variants. Consequently, this activator is a suitable candidate for the development of a pharmacological chaperone specific for PMM2-CDG. Furthermore, this molecule is naturally present in the cells, where it is hydrolyzed by a paralog of PMM2, phosphomannomutase-1 (PMM1, Q92871). Despite its name and structural similarity with PMM2, the paralog physiologically acts as a bisphosphatase, rather than a phosphomannomutase. In 2008, Veiga-da-Cunha and co-workers matched the identity of the well-known IMP-stimulated brain Glc-1,6-bisphosphatase with that of PMM1, which they defined “an enzyme of mysterious physiological function sharing several properties with Glc-1,6-bisphosphatase” [23]. As well described by Quental and co-workers, the duplication event leading to the development of two separated genes occurred very early in vertebrate evolution [24]. Interestingly, the enzymes have different tissue distribution patterns, with ubiquitous PMM2 and mainly brain expressing PMM1. Analysis of the tissue distribution of phosphomannomutases during murine brain development highlighted an overlapping expression pattern in the brain, and these data together with the absence of compensation by PMM1 in PMM2-CDG, led the authors to suggest that “Pmm1 in vivo does not exert the phosphomannomutase-like activity seen in biochemical assays, but either acts on as yet unidentified specific substrates or fulfils entirely different functions.” [25].

The research on PCs likely starts by the analysis of natural ligands, such as the α -G16.

Given the leading role of PMM1 in hydrolyzing α -G16, two potential approaches to stabilize PMM2 have been investigated. The first one involves using a non-hydrolyzable pharmacological chaperone. To explore the viability of this strategy, we synthesized beta-glucose-1,6-bisphosphate (β -G16), a structural analog of α -G16²² - notably, β -G16 is a poor substrate for PMM1. The second strategy could be finding a selective inhibitor of PMM1, thus reducing the α -G16 hydrolysis. In light of their similarity to pyrophosphate, we turned to bisphosphonates, a class of molecules where the phosphate groups are linked to a central carbon with a non-hydrolyzable bond. Moreover, with the aim of reducing the time needed to pass from bench to bedside, we repurposed FDA-approved drugs and found a good hit in Clodronate [26].

Here, we apply the recently published ReBaTSA, to assess the binding capacity of drugs for PMM2-CDG to the proteins PMM1 and PMM2. This method circumvents the need for costly protein detection typically required in standard CeTSA and eliminates the necessity for protein purification, as in the case of Thermal Shift Assay, while still delivering comparable results.

2. Material and methods

2.1. ReBaTSA

ReBaTSA was conducted using clear protein extracts of *E. coli* BL21(DE3) expressing wt-PMM1, QDK-PMM1 or wt-PMM2. QDK-PMM1 is a PMM1 mutant which harbours mutations in the three amino acids of the active site that are not conserved (M186Q, N218D, E219K) in PMM2. These mutations are responsible for the functional differences between the paralogous enzymes. Protein expression and preparation of clear protein extract were performed as previously described [22]. ReBaTSA protocol described in Ref. [5] was used to determine the melting temperatures; alternatively, Isothermal ReBaTSA was conducted at a fixed temperature.

2.2. Enzymatic activity assays

The activity assays were performed on clear bacterial extracts hyper-expressing wt-PMM1 or wt-PMM2 in 20 mM Hepes pH 7.5 5 mM MgCl₂ at 37 °C. Phosphomannomutase activity assays were performed by continuous incubation of the extract in a mixture containing 3.7 U/mL phosphoglucoisomerase (from rabbit muscle, Sigma-Aldrich), 0.003 mg/mL phosphomannoisomerase (from *E. coli*, Sigma-Aldrich), 2.6 U/mL glucose-6-phosphate dehydrogenase (from yeast, Alfa Aesar), 0.25 mM NADP⁺ (Sigma-Aldrich), 0.2 mM mannose-1-phosphate (Sigma-Aldrich) and 0.02 mM glucose-1,6-bisphosphate (Sigma-Aldrich), in the presence of 0.1 mg/mL bovine serum albumin. NADP⁺ reduction to NADPH was followed spectrophotometrically at 340 nm. Clodronate concentration was 2.8 mM.

Phosphoglucomutase activity assays were performed by continuous incubation of the extract in a mixture containing 2.6 U/mL glucose-6-phosphate dehydrogenase (from yeast, Alfa Aesar), 0.25 mM NADP⁺ (Sigma-Aldrich), 0.04 mM glucose-1-phosphate (G1P, Sigma-Aldrich) and 0.03 mM glucose-1,6-bisphosphate (Sigma-Aldrich), in the presence of 0.1 mg/mL bovine serum albumin. NADP⁺ reduction to NADPH was followed spectrophotometrically at 340 nm. Clodronate concentration was 0–2.9 mM.

Phosphatase activity was performed by continuous incubation of the extract in a mixture containing 2.6 U/mL glucose-6-phosphate dehydrogenase (from yeast, Alfa Aesar), 0.034 U/mL phosphoglucomutase (from rabbit muscle, Sigma-Aldrich), 0.25 mM NADP⁺ (Sigma-Aldrich), in the presence of 0.1 mg/mL bovine serum albumin. Glucose-1,6-bisphosphate was used as a substrate in the 0.001–0.25 mM range. Clodronate concentration was 0.03–3.3 mM.

2.3. Cell cultures and quantification of α -G16 abundance

Arg141His/Phe119LeuPMM2 fibroblasts were a gift from Prof. Flemming Skovby (rigshospitalet.dk) who had obtained with informed consent from patients in accordance with The Code of Ethics of the World Medical Association (Declaration of Helsinki) [27]. Cells were cultured in RPMI medium supplemented with 10% Fetal Bovine Serum, 2 mM glutamine, 0.5 mg/mL penicillin, 0.5 mg/mL streptomycin, and non-essential amino acids at 37 °C in 5% humidified CO₂. Treatment was performed using 50 μ M clodronate for 4 h. Cells were washed twice with ice-cold PBS, and metabolites were

collected using ice-cold 5% HClO₄ and centrifuged at 9400×g at 4 °C for 15 min. Supernatant containing metabolites was neutralized with 0.5 M K₂CO₃ and centrifuged again, the protein pellet was resuspended in 0.2 M NaOH. Recovered volumes of supernatants were measured before stocking. Measurement of α-G16 abundance in the metabolite extracts was performed as previously described [28].

2.4. In silico docking

We used the structure of PMM1 deposited with the code pdb 2fue as the receptor. We prepared the pdb for docking by removing non-standard residues and adding hydrogens through the Protoss tool [29] on proteins.plus web service [30]. We separately saved relevant components of the pdb (i.e., the two Mg²⁺ atoms, the mannose-1-phosphate, and the water molecules around the catalytic Mg²⁺ atom) to use as cofactors during docking. Clodronate (pubchemid 2883804) was downloaded from ligandbox [26], protonated manually using the protonation state associated with the Clodronate drugbank entry, and saved as in ChimeraX. The docking was performed through the dockthor [27] web service with all default options except for activating blind docking mode. Docking was performed twice: once using all the cofactors and Clodronate and the other using all cofactors but mannose. When preparing the first docking, Mannose-1-phosphate (pubchemID 439279) was positioned coherently with its pose in the 2fue structure. PMM1/2fue binding pocket was downloaded from CASTp [31]. We used Chimera for all operations related to output visualization.

2.5. Molecular dynamics

GROMACS version 2022.3 was used to obtain 100 ns long trajectories, selecting the OPLS-AA force field. A cubic box was generated, with a distance of 1.3 nm set between the protein and the boundaries of the system with periodic boundary conditions.

Clodronate parameters were generated using HyperChem. The solute was solvated with the TIP3P water model, and the system's charge was neutralized using Na⁺ and Cl⁻ ions.

Following this, an energy minimization was performed using the steepest descent algorithm for a maximum of 500,000 steps. Subsequently, the two systems were equilibrated under isothermal-isovolumetric and isothermal-isobaric conditions for 1 ns each.

2.6. Data analysis and statistics

All the experiments were performed at least in duplicate. Data were analyzed using KaleidaGraph™. Two-group comparisons were performed using a Student t-test for uncoupled data with equal variance (F test was performed to confirm the equal variance). Multiple comparisons were performed using the One-Way ANOVA test with Tukey post-hoc analysis.

Melting curves were analyzed by fit of a sigmoidal curve. Melting curves shown in the Figures are representative of one experiment; melting temperatures were calculated as mean ± standard deviation of independent experiments. The complete sets of data and the statistical analysis are provided in Supplementary File 1.

3. Results and discussion

In order to conduct temperature-based drug screening using Isothermal ReBaTSA, it is necessary to determine the melting curve and identify the melting temperature (T_M) of the target protein without ligands. To that end, raw extracts of *E.coli* transformed with

expression vectors encoding PMM1 and PMM2 were incubated at different temperatures as described in the methods. Subsequently, we performed SDS-PAGE analysis and measured the intensity of the band of the PMM2 as a function of the incubation temperature. We then identified the temperature at which the band's intensity corresponding to the hyper-expressed protein was half that in the non-heated control.

We conducted the same experiment on QDK-PMM1, which contains mutations in the three amino acids of the active site that are not conserved in PMM2. These mutations are responsible for the functional differences between the paralogous enzymes. Fig. 1 depicts the melting profiles for the three proteins. The wild-type PMM2 had a T_M of 51.0 ± 1.1, the wild-type PMM1 of 46.2 ± 0.7 °C, while QDK-PMM1 had a T_M of 42.9 ± 1.4 °C.

We analyzed the effects of three drugs: β-G16, Clodronate, and Neridronate. The experiments were conducted at 46 °C for wt-PMM1, 43 °C for QDK-PMM1, and 52 °C for wt-PMM2 - temperatures slightly higher than the T_M for the apo-state of each protein. In such an experiment, differences in the relative band intensities with or without a ligand provide evidence of protein-ligand binding. Fig. 2 (panels A, B, and C) shows that the relative band intensity associated with β-G16 significantly increases with respect to the no ligand for all of the proteins, suggesting the ligand can bind and stabilize the three of them. Neridronate does not bind to any of them (i.e., no significant increase in band intensity if comparing the neridronate data with the no ligand), whereas Clodronate has a specific effect on wt-PMM1. In fact, wt-PMM1 clodronate related band intensities are significantly higher if compared to the no ligand, whereas for QDK-PMM1 and wt-PMM2 there is no difference whether the proteins were incubated with clodronate or with no ligand.

To validate the effects of Clodronate, we carried out two sets of experiments, incubating *E. coli* expressing wt-PMM1 at different

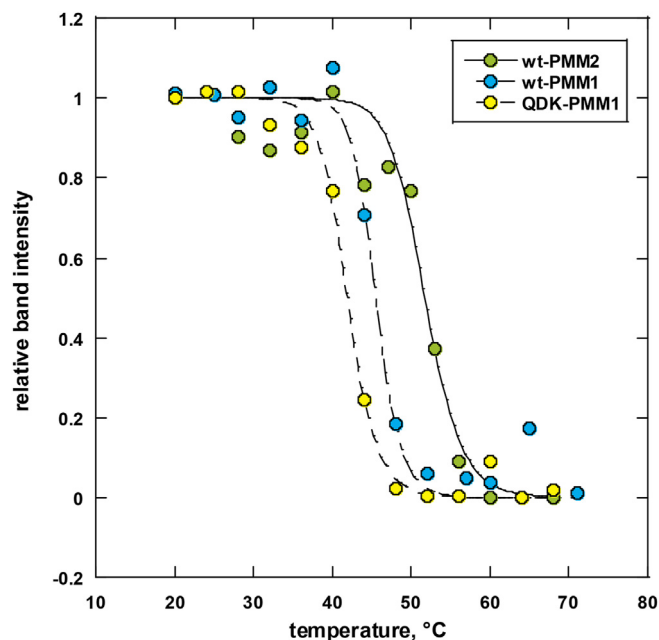


Fig. 1. Melting profiles of wt-PMM2, wt-PMM1, and QDK-PMM1. Proteins were hyper-expressed in *E. coli*, and ReBaTSA protocol was applied to clear bacterial extracts, followed by SDS-PAGE visualization. Quantitative analysis of bands was performed to determine the melting temperature. Melting temperatures were calculated as a mean of independent experiments (complete data sets are provided in Supplementary File 1). The T_M was 51.0 ± 1.1 °C for wt-PMM2 (n = 2), 46.2 ± 0.7 °C for wt-PMM1 (n = 3) and 42.9 ± 1.4 °C for QDK-PMM1 (n = 2).

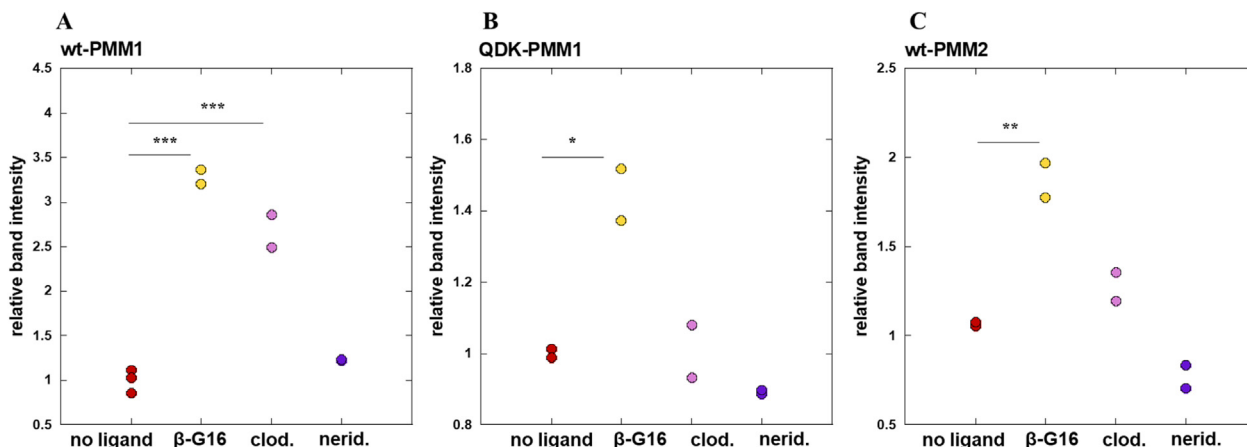


Fig. 2. Drug screening on wt-PMM1, QDK-PMM1 and wt-PMM2.

Isothermal ReBaTSA was performed at the melting temperature (46 °C for wt-PMM1, 43 °C for QDK-PMM1 and 52 °C for wt-PMM2). Raw bacterial extracts hyper-expressing the proteins of interest were incubated for 4 min in the presence of 1 mM β -G16, Clodronate (clod.), or Neridronate (nerid.). Samples were centrifuged at 18,400 \times g for 10' at 4 °C, and supernatants were analyzed via SDS-PAGE. Drugs' effects were evaluated using the Tukey post-hoc test (* = $p < 0.05$, ** = $p < 0.01$, *** = $p < 0.001$; $n = 2$). Significance evaluated for all possible drug/no_ligand pairs are reported; a full table with all results of statistical tests is available as Supplementary File 1.

temperatures in the presence or absence of the ligand. The maximal effect on T_M was observed when wt-PMM1 was incubated with 2.8 mM Clodronate (Fig. 3, panel A), and T_M increased to 49.9 ± 1.7 °C. The effect of Clodronate on T_M is dose-dependent and specific since no statistically significant augment was recorded for PMM2 in the same range of concentrations (Fig. 3, panel B). Calculation of EC50 by interpolation of the dose-response curve for wt-PMM1 resulted in 0.34 ± 0.12 mM.

To assess the specificity of the effect on catalysis, we analyzed the effect of the drug on the isomerization of mannose-1-phosphate, an activity that PMM2 and, to a lesser extent, PMM1 manifest. Clodronate inhibited wt-PMM1 (Fig. 4, panel A) activity but not wt-PMM2 (Fig. 4, panel B). The mechanism of action of Clodronate was investigated using PMM1 bisphosphatase activity

as a function of the substrate concentration, aG16, and of the inhibitor concentration, Clodronate. Clodronate acts as a PAM-antagonist (Positive Allosteric Modulator-Antagonist), producing a sinistral displacement of curves and depression of maxima (Fig. 4, panel C) [32].

Kinetic parameters associated with the bisphosphatase activity were extracted by fitting the data to the Hill equation. Hill coefficient (nH), the maximal velocity (V_{max}), and the substrate concentrations giving 50% of the maximal velocity ($S_{0.5}$) were as follow: 3.31 ± 0.96 , 0.96 ± 0.05 U/mg, 33.33 ± 2.68 μ M at 0 mM clodronate; 1.17 ± 0.35 , 0.50 ± 0.04 U/mg, 12.21 ± 3.44 microM at 3.33 mM clodronate.

Data obtained using 0.04 mM a-G16 as a substrate were extrapolated to compare the inhibitory effect on bisphosphatase

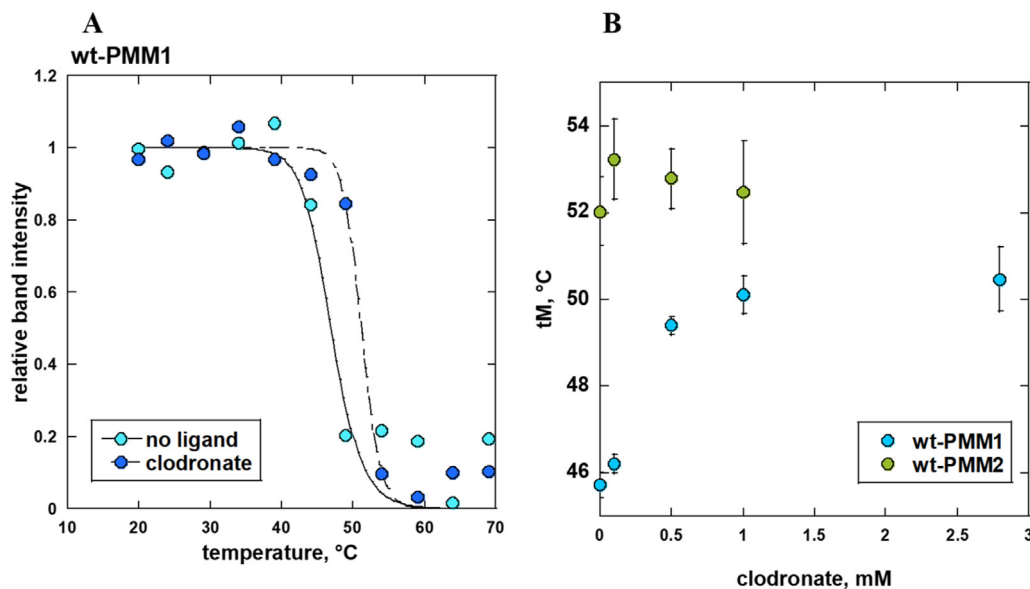


Fig. 3. wt-PMM1 melting curve in the presence of Clodronate and dose-response.

Panel A. ReBaTSA on wt-PMM1 in the presence or the absence of 2.8 mM Clodronate. The melting temperature increased from 46.2 ± 0.7 °C to 49.9 ± 1.7 °C. Melting temperatures were calculated as a mean of independent experiments (complete data sets are provided in Supplementary File 1). Panel B. Dose-responsiveness of wt-PMM1 to Clodronate binding. The melting temperatures of wt-PMM1 and wt-PMM2 in the presence of increasing concentrations of Clodronate were determined using a ReBaTSA protocol. Clodronate specifically binds wt-PMM1.

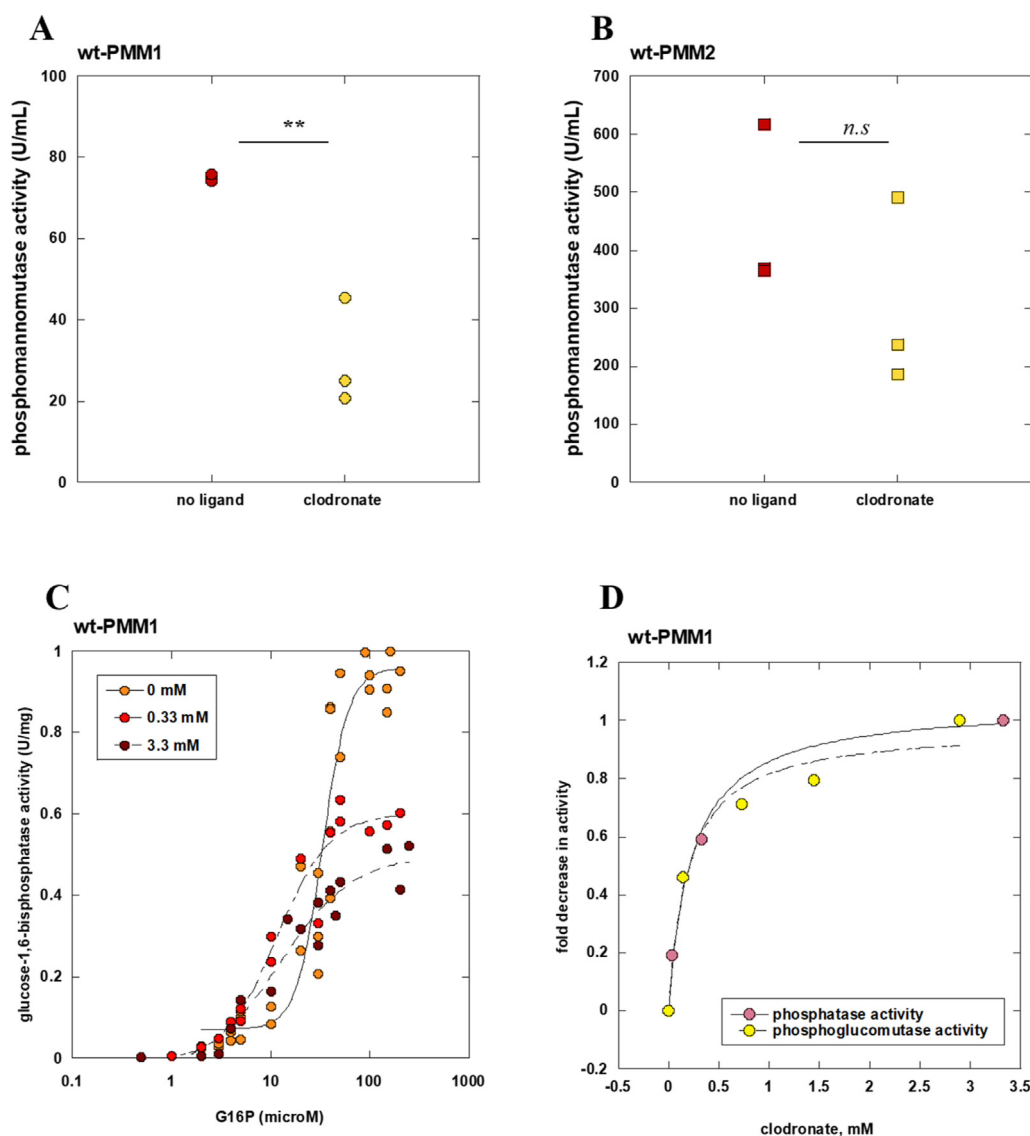


Fig. 4. Phosphomannomutase and phosphatase activity in the presence of Clodronate.

Panels A and B. Phosphomannomutase activity in the presence of Clodronate. PMM activity of wt-PMM1 (A) and wt-PMM2 (B) with or without 2.8 mM Clodronate was determined using a coupled enzymatic activity assay in the presence of 3.7 U/mL phosphoglucoisomerase, 0.003 mg/mL phosphomannoisomerase, 2.6 U/mL glucose-6-phosphate dehydrogenase, 0.25 mM NADP⁺, 0.2 mM M1P and 0.02 mM α -G16. A Student t-test for uncoupled data with equal variance was used to evaluate the differences in the treatments (** = $p < 0.01$, $n = 3$). Panels C and D. In panel C, phosphatase activity of wt-PMM1 measured in the presence of growing concentrations of Clodronate (0–3.3 mM) with different concentrations of glucose-1,6-bisphosphate (0–250 μ M) as substrate. In panel D, comparison of fold-decrease in phosphatase (a-G16 0.04 mM) and phosphoglucomutase activity (G1P 0.04 mM).

activity with that on phosphoglucomutase activity (Fig. 4, panel D), and the EC₅₀ was calculated for both, resulting in $0,23 \pm 0,06$ mM for bisphosphatase and $0,20 \pm 0,07$ mM for phosphoglucomutase. These data perfectly align with those obtained by interpolation of the dose-response curve in Fig. 3, panel B.

ReBaTSA on wt-PMM1 was performed in the presence of different ligands, in order to explore which PMM1 form was more likely to bind clodronate (Supp Fig. 1). Results show the strongest stabilization by M1P, as expected. Interestingly, M1P-bound PMM1 was still able to bind clodronate, resulting in a lowered stabilizing effect. *In silico* docking and molecular dynamics helped deepening these results.

The PMM1 crystal structure is available in PDB as 2fue. Starting from the pdb file, we removed non-standard residues and added the hydrogens, then used this structure for *in silico* docking through the dockthor [33] web service. As shown in Fig. 5 panel A, when the

binding pocket was full with M1P, Clodronate was posed around the non-catalytic Mg²⁺. Conversely, if the pocket is free, Clodronate occupies it (Fig. 5, panel B).

As reported in Fig. 5, Met186 is less than 4 Å far from Clodronate among the interacting amino acids. This event is interesting since Met186 is mutated to Gln in our QDK-PMM1, which is unresponsive to Clodronate. Based on the above results, we hypothesize that Met186 is crucial in determining the different responses to Clodronate of PMM1 and PMM2.

In silico docking of clodronate shows how it can accommodate itself in the binding site when it is the only ligand, or near the structural magnesium when present simultaneously with M1P.

Molecular dynamics simulations starting from the crystallographic structures used as docking inputs (trj1, trj2; respectively empty structure (2fuc) and with M1P in the binding site (2fue)), from the best PMM1-clodronate docking pose (trj3), from a

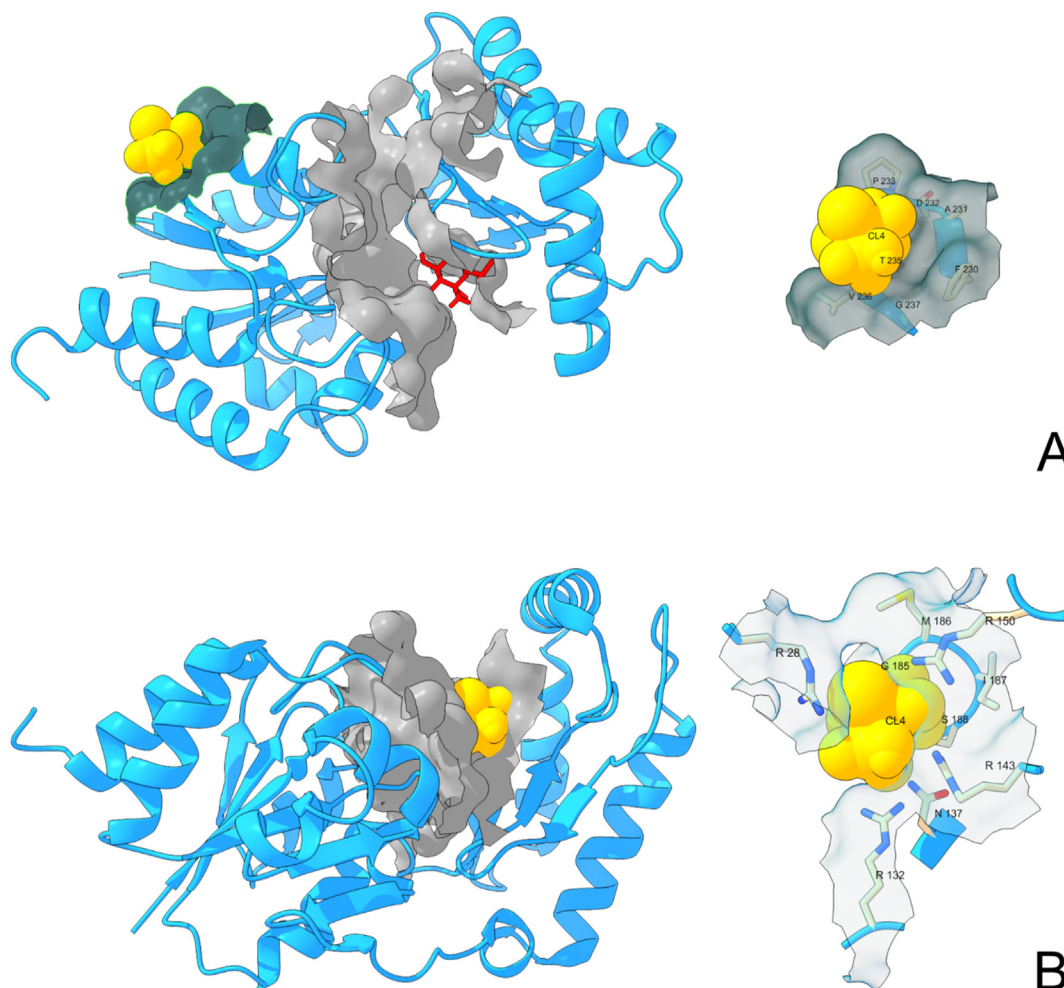


Fig. 5. *In silico* docking of wt-PMM1 with Clodronate. 2fue crystallographic structure was modified as described in the Methods and used to perform *in silico* docking with Clodronate using the dockthor web services. Panel A. Docking was performed with the binding pocket (gray) full with M1P (red); Clodronate (light orange) is placed near residues coordinating with the non-catalytic Mg^{2+} (surface in dark gray). Panel B. Docking in the presence of an M1P-free binding site. Clodronate (light orange) enters with the binding pocket (gray) and is positioned at less than 4 Å distance from the following amino acids (inset): Arg132, Arg143, Arg150, Arg28, Ile187, Met186, and Ser188. Met186 is particularly interesting since it is mutated in the QDK-PMM1, which does not bind Clodronate.

situation where clodronate is near the binding site occupied by M1P (trj4) and from the best pose for docking of clodronate when mannose occupies the binding site (trj5) allow investigating the stability of the protein in each of these situations. *In silico* trajectories are consistent with the *in vitro* results.

The trajectory of the PMM1-clodronate pose supports the docking results and highlights the ligand's ability to stabilize the protein. Clodronate remains within a restricted vicinity of the position predicted by docking (stable and low RMSD, green line in Fig. 6B). At the same time, analyzing the RMSF (green line, Fig. 6D), we notice that the protein with the ligand lodged in the catalytic pocket (green line) is comparable in mobility to the protein complexed with M1P (blue line) but less mobile compared to the protein in the absence of ligand (red line).

The comparison of trajectories 2 and 3 (PMM1-CL4 and PMM1-M1P) confirms what the ReBaTSA shows: M1P stabilizes the protein structure better than clodronate. The RMSD deviations of PMM1-CL4 (Fig. 6A, green line) are larger than those of PMM1-M1P (blue line), where the radius of gyration of PMM1-M1P is smaller (Fig. 6C, same colors).

The trajectory in which the two ligands appear simultaneously, and the clodronate is in the neighborhood of the catalytic pocket,

suggests the inability of clodronate to displace mannose from the binding site. The joint analysis of backbone and ligand RMSD shows that mannose moves little (reduced fluctuations of the solid orange line, Fig. 6B), whereas the position of the clodronate tends to vary more. Furthermore, the simultaneous presence of the two ligands within the catalytic pocket impacts the compactness of the protein (sustained fluctuations in the radius of gyration; orange line in Fig. 6C) and increases its mobility compared to the other cases (wider variations in the RMSF, orange line in Fig. 6D).

The fifth trajectory (trj5), starting from the best docking pose with clodronate and M1P, produces a stable structure comparable to the PMM1-M1P trajectory, as we can see from deviation in Fig. A and from the M1P RMSD in Fig. B (in both cases similar for purple and blue lines). During the trajectory, the clodronate carries the Mg^{2+} ion away from the protein (Supp. Fig. 2) and the compactness of the latter increases (Fig. 6C, purple line; for this reason, the CL4 is not represented in Fig. 6B). The *in silico* behavior of clodronate is consistent with experimental observations of its chelating ability [34].

To further validate the potential of Clodronate as a lead compound to inhibit bisphosphatase activity in cells, we treated PMM2-CDG patient-derived fibroblasts carrying $Arg^{141}His/Phe^{119}Leu$ PMM2.

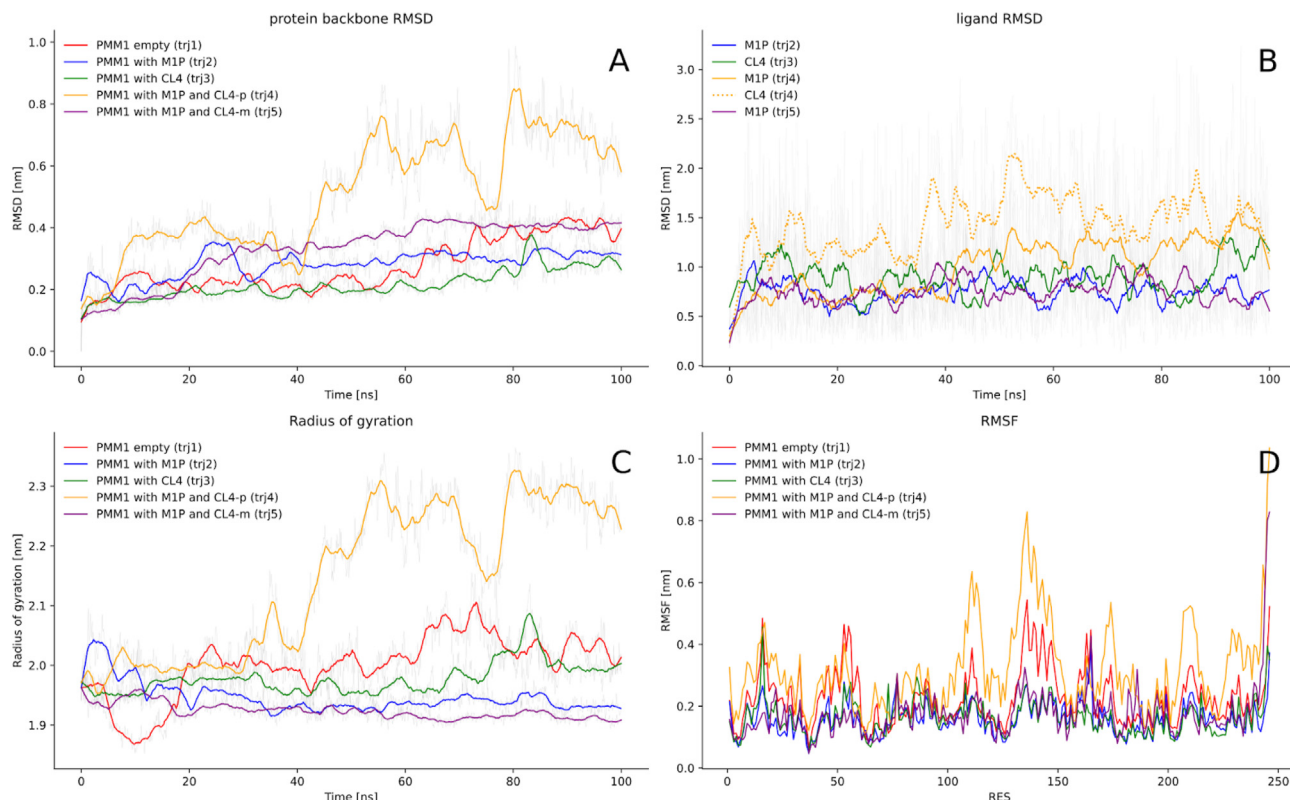


Fig. 6. Analysis of molecular dynamics trajectories for unbound and complexed PMM1. A. root mean square deviation (RMSD) of the protein backbone from the starting frame; B. RMSD of the ligand from the starting frame, with reference to the entire system; C. radius of gyration of the protein during the trajectory; D. per-residue root mean square fluctuation (RMSF) of the protein. Different colors indicate value smoothing for different structures as per legend; different line types in panel B indicate different ligands in the same structure. Acronyms: PMM1: Phosphomannomutase 1; MP1: Mannose-1-Phosphate; CL4: Clodronate; CL4-p: pose with clodronate around the catalytic pocket; CL4-m: pose with clodronate around the Structural Magnesium.

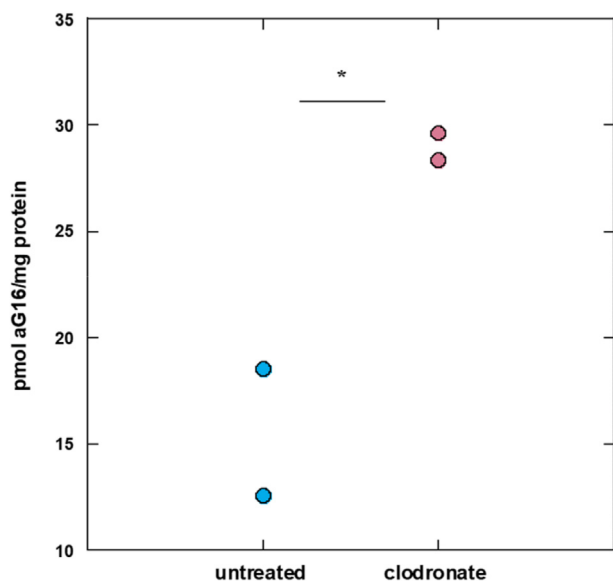


Fig. 7. Increase in intracellular α -G16 upon clodronate treatment. PMM2-CDG patient-derived fibroblasts (Arg141His/Phe119LeuPMM2) were treated with 0.05 mM clodronate for 4 h, then metabolites were extracted using a perchloric acid protocol, and the content of α -G16 was analyzed enzymatically, relying on the increase in phosphoglucomutase activity in the presence of increasing concentrations of α -G16. A Student t-test for uncoupled data with equal variance was used to evaluate the differences in the treatments (* = $p < 0.05$, $n = 2$).

As shown in Fig. 7, a 4 h treatment with 0.05 mM clodronate resulted in a significant increase in the intracellular α -G16.

4. Conclusions

A cure for the life-threatening disease PMM2-CDG currently has not been described but various therapeutic strategies have been proposed to augment phosphomannomutase activity within cells. Among them, stabilizing PMM2 through binding by pharmacological chaperones can boost the protein's cellular levels. Additionally, inhibiting PMM1's phosphatase activity can elevate the intracellular levels of α -G16, enhancing PMM2 activity.

In this study, we applied a simplified CeTSA protocol for drug screening (named ReBaTSA), which confirmed the binding of the substrate analog β -G16 to both wt-PMM1 and wt-PMM2. As β -G16 binds to the protein and is known to be minimally hydrolyzed by PMM1, it emerges as a potential lead compound for the formulation of a pharmacological chaperone targeting PMM2.

Among the ligands screened, Clodronate — a bisphosphonate typically prescribed for osteoporosis in postmenopausal women, malignant hypercalcemia, and osteolysis [35] — garnered our attention. Previous studies identified Clodronate as a selective inhibitor of PMM1's phosphatase activity. Using the ReBaTSA protocol, we demonstrated Clodronate's specific binding affinity to PMM1, the dose-responsive nature of this binding, and the resultant inhibition of phosphomannomutase activity in PMM1 but not in PMM2. To further probe the interaction between Clodronate and PMM1, we employed a triple mutant (QDK-PMM1), which showed no affinity for Clodronate. This mutant harbors alterations in the

active site, specifically in three non-conserved amino acids. One amino acid, Met186, was pinpointed as a pivotal player in ligand binding through *in silico* docking. We achieved a greater level of inhibition of the PMM1 bisphosphatase activity and identified Clodronate acts as a Positive Allosteric Modulator-Antagonist. This result was supported by *in silico* experiments that suggest that Clodronate is not able to displace physiological ligands and could act as allosteric inhibitor by affecting protein stability when M1P occupies the active site. Notwithstanding the high concentrations needed to achieve bisphosphatase inhibition, clodronic acid is reported as having “a wide therapeutic index as a large overdose is required for significant toxicity” [35]. When exploring the effects of clodronate treatments on PMM2-CDG patient-derived fibroblasts, by evaluating the a-G16 content in a metabolite extract, we observed that a-G16 increases upon a 4-h treatment, pointing at the clodronate as a promising lead compound in drug discovery for PMM2-CDG.

In conclusion, PMM1 functionally plays a direct role in PMM2-CDG by diminishing the availability of α -G16 for PMM2. Our findings emphasize that the structural distinctions between phosphomannosidases are vital in directing drug discovery efforts for PMM2-CDG.

Funding

We acknowledge the funding by the Italian Ministry of University and Research PRIN 2022B2N2BY.

Acknowledgements

We acknowledge the National Research Council of Italy, Joint Bilateral Agreement CNR/Slovak Academy of Sciences, Biennial program 2023–24.

Appendix A. Supplementary data

Supplementary data to this article can be found online at <https://doi.org/10.1016/j.biochi.2024.02.011>.

References

- [1] L. Liguori, M. Monticelli, M. Allocca, et al., Pharmacological chaperones: a therapeutic approach for diseases caused by destabilizing missense mutations, *Int. J. Mol. Sci.* 21 (2) (2020), <https://doi.org/10.3390/ijms21020489>.
- [2] G. Andreotti, M. Monticelli, M.V. Cubellis, Looking for protein stabilizing drugs with thermal shift assay, *Drug Test. Anal.* 7 (9) (2015), <https://doi.org/10.1002/dta.1798>.
- [3] T.A. Tolvanen, Current advances in CETSA, *Front. Mol. Biosci.* 9 (2022) 866764, <https://doi.org/10.3389/fmolb.2022.866764>.
- [4] G. Parenti, G. Andria, K.J. Valenzano, Pharmacological chaperone therapy: preclinical development, clinical translation, and prospects for the treatment of lysosomal storage disorders, *Mol. Ther.* 23 (7) (2015) 1138–1148, <https://doi.org/10.1038/mt.2015.62>.
- [5] M. Monticelli, D.M. Wright, M.V. Cubellis, G. Andreotti, ReBaTSA: a simplified CeTSA protocol for studying recombinant mutant proteins in bacterial extracts, *Biochim. Biophys. Acta Gen. Subj.* 1868 (2) (2024) 130526, <https://doi.org/10.1016/j.bbagen.2023.130526>.
- [6] J. Jaeken, J. Artigas, R. Barone, et al., Phosphomannosidase deficiency is the main cause of carbohydrate-deficient glycoprotein syndrome with type I isoelectrofocusing pattern of serum sialotransferrins, *J. Inher. Metab. Dis.* 20 (1997), <https://doi.org/10.1023/A:1005331523477>.
- [7] S. Grünewald, The clinical spectrum of phosphomannosidase 2 deficiency (CDG-1a), *Biochim. Biophys. Acta (BBA) - Mol. Basis Dis.* (9) (2009) 1792, <https://doi.org/10.1016/j.bbadis.2009.01.003>.
- [8] M.L. Monin, C. Mignot, P. De Lonlay, et al., 29 French adult patients with PMM2-congenital disorder of glycosylation: outcome of the classical pediatric phenotype and depiction of a late-onset phenotype, *Orphanet J. Rare Dis.* 9 (2014), <https://doi.org/10.1186/s13023-014-0207-4>.
- [9] M. Serrano, V. De Diego, J. Muchart, et al., Phosphomannosidase deficiency (PMM2-CDG): ataxia and cerebellar assessment, *Orphanet J. Rare Dis.* 10 (1) (2015), <https://doi.org/10.1186/s13023-015-0358-y>.
- [10] G. Matthijs, E. Schollen, C. Bjursell, et al., Mutations in PMM2 that cause congenital disorders of glycosylation, type Ia (CDG-1a), *Hum. Mutat.* 16 (5) (2000) 386–394, [https://doi.org/10.1002/1098-1004\(200011\)16:5<386::AID-HUMU2>3.0.CO;2-Y](https://doi.org/10.1002/1098-1004(200011)16:5<386::AID-HUMU2>3.0.CO;2-Y).
- [11] G. Matthijs, E. Schollen, E. Van Schaftingen, J.J. Cassiman, J. Jaeken, Lack of homozygotes for the most frequent disease allele in carbohydrate-deficient glycoprotein syndrome type 1A, *Am. J. Hum. Genet.* 62 (3) (1998) 542–550, <https://doi.org/10.1086/301763>.
- [12] E. Schollen, S. Kjaergaard, E. Legius, M. Schwartz, G. Matthijs, Lack of Hardy-Weinberg equilibrium for the most prevalent PMM2 mutation in CDG-1a (congenital disorders of glycosylation type Ia), *Eur. J. Hum. Genet.* 8 (5) (2000), <https://doi.org/10.1038/sj.ejhg.5200470>.
- [13] A.I. Vega, C. Pérez-Cerdá, D. Abia, et al., Expression analysis revealing destabilizing mutations in phosphomannosidase 2 deficiency (PMM2-CDG): expression analysis of PMM2-CDG mutations, *J. Inher. Metab. Dis.* 34 (4) (2011), <https://doi.org/10.1007/s10545-011-9328-2>.
- [14] S. Kjaergaard, F. Skovby, M. Schwartz, Absence of homozygosity for predominant mutations in PMM2 in Danish patients with carbohydrate-deficient glycoprotein syndrome type 1, *Eur. J. Hum. Genet.* 6 (4) (1998) 331–336, <https://doi.org/10.1038/sj.ejhg.5200194>.
- [15] G. Andreotti, M.C. Monti, V. Citro, M.V. Cubellis, Heterodimerization of two pathological mutants enhances the activity of human phosphomannosidase 2, *PLoS One* 10 (10) (2015), <https://doi.org/10.1371/journal.pone.0139882>.
- [16] C. Le Bizet, S. Vuillaumier-Barrot, A. Barnier, T. Dupré, G. Durand, N. Seta, A new insight into PMM2 mutations in the French population, *Hum. Mutat.* 25 (5) (2005) 504–505, <https://doi.org/10.1002/humu.9336>.
- [17] S. Vuillaumier-Barrot, G. Hetet, A. Barnier, et al., Identification of four novel PMM2 mutations in congenital disorders of glycosylation (CDG) Ia French patients, *J. Med. Genet.* 37 (8) (2000) 579–580, <https://doi.org/10.1136/jmg.37.8.579>.
- [18] P. Yuste-Checa, A. Gámez, S. Brasil, et al., The effects of PMM2-CDG-causing mutations on the folding, activity, and stability of the PMM2 protein, *Hum. Mutat.* 36 (9) (2015) 851–860, <https://doi.org/10.1002/humu.22817>.
- [19] M. Pirard, G. Matthijs, L. Heykants, et al., Effect of mutations found in carbohydrate-deficient glycoprotein syndrome type IA on the activity of phosphomannosidase 2, *FEBS Lett.* 452 (3) (1999) 319–322, [https://doi.org/10.1016/s0014-5793\(99\)00673-0](https://doi.org/10.1016/s0014-5793(99)00673-0).
- [20] G. Andreotti, I.C. De Vaca, A. Poziello, M.C. Monti, V. Guallar, M.V. Cubellis, Conformational response to ligand binding in Phosphomannosidase 2: insights into inborn glycosylation disorder, *J. Biol. Chem.* 289 (50) (2014), <https://doi.org/10.1074/jbc.M114.586362>.
- [21] G. Andreotti, E. Pedone, A. Giordano, M.V. Cubellis, Biochemical phenotype of a common disease-causing mutation and a possible therapeutic approach for the phosphomannosidase 2-associated disorder of glycosylation, *Mol. Genet. Genom. Med.* 1 (1) (2013), <https://doi.org/10.1002/mgg3.3>.
- [22] M. Monticelli, L. Liguori, M. Allocca, G. Andreotti, M.V. Cubellis, β -Glucose-1,6-Bisphosphate stabilizes pathological phosphomannosidase 2 mutants in vitro and represents a lead compound to develop pharmacological chaperones for the most common disorder of glycosylation, PMM2-CDG, *Int. J. Mol. Sci.* 20 (17) (2019), <https://doi.org/10.3390/ijms20174164>.
- [23] M. Veiga-Da-Cunha, W. Vleugels, P. Maliekal, G. Matthijs, E. Van Schaftingen, Mammalian phosphomannosidase PMM1 is the brain IMP-sensitive glucose-1,6-bisphosphatase, *J. Biol. Chem.* 283 (49) (2008), <https://doi.org/10.1074/jbc.M805224200>.
- [24] R. Quental, A. Moleirinho, L. Azevedo, A. Amorim, Evolutionary history and functional diversification of phosphomannosidase genes, *J. Mol. Evol.* 71 (2) (2010), <https://doi.org/10.1007/s00239-010-9368-5>.
- [25] K. Cromphout, L. Keldermans, A. Snellinx, et al., Tissue distribution of the murine phosphomannosidases Pmm1 and Pmm2 during brain development, *Eur. J. Neurosci.* 22 (4) (2005) 991–996, <https://doi.org/10.1111/j.1460-9568.2005.04266.x>.
- [26] V. Citro, C. Cimmaruta, L. Liguori, G. Viscido, M.V. Cubellis, G. Andreotti, A mutant of phosphomannosidase 1 retains full enzymatic activity, but is not activated by IMP: possible implications for the disease PMM2-CDG, *PLoS One* 12 (12) (2017), <https://doi.org/10.1371/journal.pone.0189629>.
- [27] S. Kjaergaard, F. Skovby, M. Schwartz, Carbohydrate-deficient glycoprotein syndrome type 1A: expression and characterisation of wild type and mutant PMM2 in *E. coli*, *Eur. J. Hum. Genet.* 7 (8) (1999), <https://doi.org/10.1038/sj.ejhg.5200398>.
- [28] R.C. Vignogna, M. Allocca, M. Monticelli, et al., Evolutionary rescue of phosphomannosidase deficiency in yeast models of human disease, *Elife* 11 (2022), <https://doi.org/10.7554/eLife.79346>.
- [29] S. Bietz, S. Urbaczek, B. Schulz, M. Rarey, Protoss: a holistic approach to predict tautomers and protonation states in protein-ligand complexes, *J. Cheminf.* 6 (1) (2014) 12, <https://doi.org/10.1186/1758-2946-6-12>.

- [30] K. Schöning-Stierand, K. Diedrich, C. Ehrh, et al., ProteinsPlus: a comprehensive collection of web-based molecular modeling tools, *Nucleic Acids Res.* 50 (W1) (2022) W611–W615, <https://doi.org/10.1093/nar/gkac305>.
- [31] W. Tian, C. Chen, X. Lei, J. Zhao, J. Liang, CASTp 3.0: computed atlas of surface topography of proteins, *Nucleic Acids Res.* 46 (W1) (2018) W363–W367, <https://doi.org/10.1093/nar/gky473>.
- [32] T.P. Kenakin, Chapter 5 - allosteric drug effects, in: T.P. Kenakin (Ed.), *Pharmacology in Drug Discovery and Development*, second ed., Academic Press, 2017, pp. 101–129, <https://doi.org/10.1016/B978-0-12-803752-2.00005-3>.
- [33] DockThor. Accessed October 17, 2023. <https://dockthor.lncc.br/v2/index.php>.
- [34] P.P. Wright, C. Cooper, B. Kahler, L.J. Walsh, From an assessment of multiple chelators, clodronate has potential for use in continuous chelation, *Int. Endod. J.* 53 (1) (2020) 122–134, <https://doi.org/10.1111/iej.13213>.
- [35] Clodronic acid. Accessed October 19, 2023. <https://go.drugbank.com/drugs/DB00720>.